

ACCEPTED VERSION

Ka Lok Lee, Alfonso Chinnici, Mehdi Jafarian, Maziar Arjomandi, Bassam Dally, Graham Nathan
The influence of wall temperature distribution on the mixed convective losses from a heated cavity

Applied Thermal Engineering, 2019; 155:157-165

© 2019 Elsevier Ltd. All rights reserved.

This manuscript version is made available under the CC-BY-NC-ND 4.0 license

<http://creativecommons.org/licenses/by-nc-nd/4.0/>

Final publication at <http://dx.doi.org/10.1016/j.applthermaleng.2019.03.052>

PERMISSIONS

<https://www.elsevier.com/about/policies/sharing>

Accepted Manuscript

Authors can share their [accepted manuscript](#):

24 Month Embargo

After the embargo period

- via non-commercial hosting platforms such as their institutional repository
- via commercial sites with which Elsevier has an agreement

In all cases [accepted manuscripts](#) should:

- link to the formal publication via its DOI
- bear a CC-BY-NC-ND license – this is easy to do
- if aggregated with other manuscripts, for example in a repository or other site, be shared in alignment with our [hosting policy](#)
- not be added to or enhanced in any way to appear more like, or to substitute for, the published journal article

10 June 2021

<http://hdl.handle.net/2440/125936>

The influence of wall temperature distribution on the mixed convective losses from a heated cavity

Ka Lok Lee, Alfonso Chinnici, Mehdi Jafarian, Maziar Arjomandi, Bassam Dally, Graham Nathan

School of Mechanical Engineering, The University of Adelaide, SA 5005, Australia

E-mail address: ka.lee@adelaide.edu.au (K.L. Lee)

Authors email:

alfonso.chinnici@adelaide.edu.au (A. Chinnici)

mehdi.jafarian@adelaide.edu.au (M. Jafarian)

maziar.arjomandi@adelaide.edu.au (M. Arjomandi)

bassam.dally@adelaide.edu.au (B.B Dally)

graham.nathan@adelaide.edu.au (G.J. Nathan)

Abstract

An experimental investigation is presented of the effects of wind speed (0 - 9 m/s), yaw angle (0° and 90°), and tilt angle (15° and -90°) on the mixed convective heat losses from a cylindrical cavity heated with different internal wall temperature distributions. The internal wall comprised 16 individually controlled heating elements to allow the distribution of the surface temperature to be well controlled, while the air flow was controlled with a wind tunnel. It is found that temperature distribution has a strong influence on the convective heat losses, with a joint dependence on the wind speed and its direction. For the no-wind and side-on wind conditions, the measured range of the heat losses varied by up to 50% with a change in the wall temperature distribution. However, for high head-on wind speeds, this variation reduced down to ~20%. In addition, the heat losses from downward tilted were ~3 times larger than the upward facing heated cavity for high wind speeds (typical of tower-mounted and beam-down configurations, respectively). Also, the measured heat losses were found to be only slightly dependent on wind speed and direction in contrast with the downward tilted cases.

Keywords

Solar Cavity Receiver; Wind; Concentrated Solar Thermal; Convective Heat Loss

32 Nomenclature

Symbols			
A	Area (m ²)	V	Wind speed (m/s)
β	Coefficient of thermal expansion (°C ⁻¹)	ν	Kinematic viscosity of air at reference temperature kg/(s.m)
D	Diameter (m)	α	Yaw angle or incoming wind direction (°)
ε	Emissivity coefficient of the internal wall surface	φ	Tilt angle of the cavity (°)
g	Gravity (m/s ²)		
Gr	Grashof number = $\frac{g\beta(T_{wall} - T_a)D_{cav}^3}{\nu^2}$	Subscript	
h_c	Convective heat transfer coefficient through the aperture (W/(m ² K))	a	Ambient
k	Thermal conductivity of air at reference temperature (W/(m. K))	as	Aspect
L	Length (m)	ap	Aperture
Nu	Nusselt number = $\frac{h_c D_{cav}}{k_{ref}}$	cav	Cavity
Q	Heat loss (W)	conv	Convection
R	Ratio	rad	Radiation
Re	Reynolds number = $\frac{VD_{cav}}{\nu}$	ref	Reference
Ri	Richardson number = $\frac{Gr}{Re^2} = \frac{g\beta(T_{wall} - T_a)D_{cav}}{V^2}$	tot	total
T	Temperature (°C)	w	Wall

34 **1 Introduction**

35 Despite the development of Concentrated Solar Thermal technologies has progressed, the
36 understanding of the influence of wall temperature distribution and wind speed on the heat
37 losses from a heated cavity remains limited. Over the last three decades, resulting in a marked
38 increase in their deployment for power generation and in the development of novel approaches
39 to utilise thermal energy for industrial processes (ASTRI 2017; Chinnici, A et al. 2016;
40 Chinnici, Alfonso et al. 2015; Chinnici, A, Nathan & Dally 2018a, 2018b; Kolb et al. 2011;
41 Philibert 2010; Tanaka 2010). The highly concentrated solar radiation, from a solar field, is
42 collected by a solar receiver, which uses a heat transfer medium to efficiently absorb the
43 radiation. Pre-commercial solar cavity receivers have been operated at temperatures on the
44 order of 1000 °C during short-term trials, which offers potential to achieve higher thermal
45 efficiency than is presently possible (Ávila-Marín, 2011; IEA-ETSAP and IRENA, 2013;
46 Lovegrove et al., 2012; Price, 2003; Segal and Epstein, 2003; Steinfeld and Schubnell, 1993).
47 However, these temperatures result in a significant increase in the heat losses (radiative and
48 convective) from the receiver relative to commercial systems. However, while it is desirable to
49 identify ways to decrease these losses, this is difficult to do because the underlying mechanisms
50 controlling them are still not well understood, especially it has been difficult to generalize the
51 findings of mix convection. Therefore, further research is required to deepen the understanding
52 of the mechanisms influencing heat losses in solar receivers and, in particular, in solar cavity
53 receivers. More specifically, new measurements are needed of the influence of the controlling
54 parameters of receiver geometry (cavity aspect ratio, aperture ratio), wind speed and direction
55 (yaw angle), cavity orientation (tilt angle), operating temperature, and wall temperature
56 distribution. The overall objective is to meet this need.

57 A detailed review of previous experimental and numerical studies of the influence of these
58 parameters on the heat losses from solar cavity receivers was reported by Ho and Iverson
59 (2014) and Wu et al. (2010). The updated review, the relation to the present and the comparison
60 between the experimental method use in different studies have been presented in the earlier
61 study from our group by Lee et al. (2018a), hence only some important reviews are highlighted
62 in the present study. The studies by Ho and Iverson (2014), Wu et al. (2010) and Lee et al.
63 (2018a) highlighted the role of wind speed and its direction and their strong influence on the
64 mixed, natural and forced convective heat losses from a cavity receiver (Mokhtar, Marwan et
65 al. 2014); (Clausing 1983; Flesch et al. 2015; Ho & Iverson 2014; Lee et al. 2018a; Ma 1993;
66 Taumoefolau et al. 2004; Wu et al. 2015). They also highlighted the strong coupling between
67 the heat losses and the geometrical features of the receiver, namely aperture and aspect ratios
68 (Ho & Iverson 2014; Lee et al. 2018b; Wu et al. 2010). In our previous work (Lee et al. 2018a,
69 2018b), we have systematically assessed the influence of wind speed, yaw angle, aperture ratio,
70 tilt angle and cavity temperature on the convective heat losses from a heated cavity facing
71 downward, for the case of a uniform temperature distribution over the surface of the cavity.
72 These recent data provide further insights into the complex heat loss phenomenon from cavity
73 receivers while also confirming trends from earlier works. However, the majority of presently
74 available data, under well-defined conditions, only consider solar cavity receivers with a
75 uniform wall temperature distribution. Although this approach simplifies the validation of
76 engineering models, in reality, solar receivers are generally characterised by a varied heat flux

77 along the walls of the cavity at different times of the day. Therefore, there is a need to better
78 understand the influence of wall temperature distribution on the heat losses for a range of
79 conditions of relevance to operation. Hence, the overall objective of the present investigation
80 is to assess the effects of the joint dependencies between temperature distribution and wind
81 speed on the heat losses through the aperture of a heated cavity receiver.

82 Understanding of the convective heat losses from cavity receivers has been advanced by the
83 numerical studies, some of which have investigated the influence of the temperature
84 distribution (uniform and non-uniform) on the radiation heat losses (Asselineau, Abbassi &
85 Pye 2014; Gil et al. 2015; Sánchez-González, Rodríguez-Sánchez & Santana 2016; Steinfeld
86 & Schubnell 1993). However, the absolute validity of these assessments is not yet known
87 because no data has previously been available with which to validate them (Flesch et al. 2014;
88 Hu et al. 2017; Lee et al. 2017; Paitoonsurikarn & Lovegrove 2003; Paitoonsurikarn, S &
89 Lovegrove 2002; Paitoonsurikarn, Sawat et al. 2011; Wu, Xiao & Li 2011; Xiao, Wu & Li
90 2012). Furthermore, most previous numerical analyses on convective heat losses have been
91 performed for a uniform wall temperature distribution, probably largely due to a lack of
92 experimental data for model validation (Ho & Iverson 2014; Stalin Maria Jebamalai 2016).
93 Therefore, the present investigation also aims to provide an experimental dataset of convective
94 heat losses from a cavity receiver with uniform and non-uniform temperature distribution,
95 under controlled conditions, to advance the development of the numerical tools needed for
96 optimisation and scale-up.

97 Advancing understanding requires spanning a range of conditions, including orientation due to
98 the dependence of natural convection on orientation. In addition, despite its lower popularity
99 relative to the tower-mounted receiver due to disadvantages of an extra surface and anticipated
100 higher cost (Kolb et al. 2011; Li, Dai & Wang 2015), the beam-down cavity solar receivers
101 have continued to receive interest due to some (at least partly) compensating advantages. These
102 include a lower wind speed and higher functionality (Leonardi 2012; Mokhtar, M 2011; Segal
103 & Epstein 2008; Wei et al. 2013). Recent studies, utilising new solar field design have also
104 reported good performance for beam-down applications (Li, Dai & Wang 2015; Mokhtar,
105 Marwan et al. 2014). One of the perceived disadvantages of the beam-down configuration is
106 the perceived high natural convective heat loss due to buoyancy (Holman 1997). On the other
107 hand, a beam-up configuration offers the advantages of a beam down without the disadvantages
108 of the secondary reflector, but at the additional cost of a taller tower. Hence all are worthy of
109 further consideration. However, no experimental measurements are available that directly
110 compare the convective heat losses from an upward facing heated cavity a downward facing
111 cavity or a downward tilted heated cavity. For these reasons, we also aim to compare the effect
112 of wind on the heat losses from a downward tilted and an upward facing receiver.

113 In light of the aforementioned gaps, the key aim of the present investigation is to provide direct
114 measurements of the influence of temperature distribution, tilt angle and wind speed on the
115 mixed convective heat losses from a solar cavity receiver. In particular, the research aims to
116 investigate; i) the effects of the temperature distribution on the convective heat losses as a
117 function of wind speed and direction; ii) the convective heat losses for an upward facing cavity
118 and a downward tilted one (15°) and its effect on the cavity's thermal performance. This

119 investigation is the first experimental study for the effect of temperature distribution on the
120 convective heat losses from a heated cavity. In this study, the effects of wind speed and cavity
121 direction on the heat losses are also presented for various temperature distribution. This is also
122 the first experimental study to investigate and compare the heat losses from the cavity receivers
123 between 2 concentrated solar technologies. The first experimental data for the convective heat
124 losses from a solar cavity receiver with various temperature distribution can be used for
125 numerical model validation, which simulate a cavity receiver heated by various solar flux
126 distribution. This is much more realistic than a cavity which assume uniform
127 temperature for the entire internal surface. The validated numerical model can be used to
128 develop a new solar cavity design for the concentrated solar system. The general finding about
129 heat loss from heated cavity from this work can also be applied to other engineering
130 applications.

131 **2 Methodology**

132 The details of the experimental arrangement used in the study have been published previously
133 by Lee et al. (2018a) so that only a brief overview is shown here. The experimental arrangement
134 has also been reported previously so that it reproduced in the supplement here (Figure S1). A
135 cavity was electrically heated and located within the open section of the University of
136 Adelaide's wind tunnel to generate negligible blockage. The external dimensions of the cavity
137 have a maximum projected area ($\sim 0.249 \text{ m}^2$) of $\sim 4.1\%$ of the wind tunnel, which has a cross-
138 sectional dimension of area $2.75 \text{ m} \times 2.19 \text{ m}$. This is approximately 330 times larger than the
139 projected area of the aperture, which is approximately 0.018 m^2). Air was used as the working
140 fluid and the velocity in the tunnel was measured using a multi-hole pressure probe from the
141 Turbulent Flow Instrumentation. K-type thermocouples are used to measure the temperature
142 and recorded by Datalogger DT85. The temperatures were feedback controlled using Matlab and
143 Simulink. The power of the heaters are controlled by the output from the Simulink to the
144 Arduino, then a DMX lighting system power controllers. Additional details of the
145 instrumentation used in this work can be found in one of our previous works (Lee et al. 2018).
146 Figure S1b presents the key dimensions of the cavity, which has an inner diameter $D_{cav} =$
147 0.3 m . The details of the method of recording the power and its errors are reported by Lee et al.
148 (2018a).

149 The influence temperature distribution on the heat losses was assessed systematically. The
150 tested conditions are shown in Table 1. This leads to a total of 112 combinations of wind speed,
151 tilt angle, yaw angle and temperature distribution. In particular, 56 combinations for the case
152 with the open aperture (to measure the convective and radiative heat losses), and 56 cases for
153 the aperture closed (to measure the heat loss through the walls). The data was recorded for each
154 heaters every time steps. However, to reduce the number of data, only the total steady state
155 power from each condition is presented in here. The powers required for each heater to maintain
156 the set point temperature are summed to be the total heat loss from the system for that condition.
157 Each condition required between 20 to 60 minutes to reach a steady state condition. Here,
158 'steady-state condition' is intended when the following conditions are satisfied for 300
159 seconds: 1) the variation of each measured temperature is below $\pm 0.5^\circ\text{C}$; and 2) the variation

160 of total heat loss is less than $\pm 5\%$ of the total power required for that condition if the total heat
 161 loss is above 2kW or $\pm 100\text{W}$ if the power is below 2kW. The mean total heat losses from the
 162 system at the steady state condition are used for this investigation.

163 Normalised heat loss for the no wind case $Q/Q_{V=0}$ was used to characterise the effect of wind
 164 on the heat loss through the aperture. This is defined as the total heat loss through the aperture
 165 relative to that for the no wind condition for various temperature distribution, as shown in Table
 166 1 and Table 2. The total heat losses through the aperture for no wind condition is the
 167 combination of convective and radiative heat loss at zero wind speed.

168 Another normalised heat loss for the uniform temperature case $Q/Q_{T=uniform}$ was used to
 169 assess the effect of temperature distribution on the heat loss through the aperture.
 170 $Q/Q_{T=uniform}$ is defined as the total heat losses through the aperture over the total heat losses
 171 through the aperture for the 300°C uniform temperature case for various wind speeds. These
 172 were performed with the average temperature of the cavity was kept constant at 300°C . Notice
 173 this, the temperatures of the heated cavity in this study are lower than the real commercial
 174 receivers. However, this study focus on the temperature distribution more than the absolute
 175 temperature. Grashof number and Richardson number should also be used to generalise the
 176 result to assess the result for other temperature and receiver size. These two non-dimensional
 177 numbers are shown to work well for varying temperature (Lee et al. 2018a), but it should be
 178 carefully validated before they are applied to a case which has different conditions.

179 The air properties, such as thermal expansion, density and kinematic viscosity, were calculated
 180 at a reference temperature T_{ref} , which is defined as

$$T_{ref} = \frac{T_w}{2} + \frac{T_a}{2}. \quad (1)$$

181 Here T_w is the internal wall temperature and T_a is the ambient temperature.

182 The main uncertainties in the instrumentation/ uncertainty term and measured data are
 183 summarised in Table 3 (in the Supplement section), the details are reported by Lee et al.
 184 (2018a). The maximum uncertainty of the power output from each heater is $\pm 25\text{W}$ ($\sim 3.1\%$ of
 185 its maximum power), which includes that from the power and temperature measurement
 186 ($\pm 0.5^\circ\text{C}$) and their effect on the feedback control system. Although the total maximum
 187 uncertainty is $\sim \pm 400\text{W}$ ($\pm 3.1\%$ of the maximum power), the average error should be much
 188 less than $\pm 3.1\%$ of the maximum power. This is because the random error is reduced by using
 189 the 16 results from the heaters ($\frac{\sqrt{16 \times \pm 25^2}}{16 \times 800} \sim \pm 0.8\%$). In addition, the uncertainty of the
 190 incoming wind speed is estimated to be $\pm 0.2\text{m/s}$.

191 **Table 1: List of experimental conditions**

Velocity V (m/s)	Yaw angle α ($^\circ$)	Tilt angle φ ($^\circ$)	Temperature of the wall T_w ($^\circ\text{C}$)	Aspect ratio $(\frac{L_{cav}}{D_{cav}})$	Aperture ratio $(\frac{D_{ap}}{D_{cav}})$
0,3,6 and 9	0	15	5 various distributions	1.5	0.0 and 0.5

0,3,6 and 9	90	15	4 various distributions	1.5	0.0 and 0.5
0,3,6 and 9	0	-90	3 various distributions	1.5	0.0 and 0.5
0	0	90	100, 200, 300 and 400	1.5	0.0 and 0.5
0	0	15	100, 200, 300 and 400	1.5	0.0 and 0.5
0	0	-90	100, 200, 300 and 400	1.5	0.0 and 0.5

192

193 The list of set point temperature for each heater position for various temperature distribution is given in Table 2, while the position can be found
 194 in the supplement Figure S2. The temperatures were firstly estimated analytically as a starting point, then the final set point temperatures were
 195 chosen based on trial and error in the experiment. This is because it is very complex to analytically estimate the temperature for various temperature
 196 distribution and wind conditions. In this study, the range of temperatures is designed to be as wide as possible with the limitation of keeping the
 197 maximum variation of the average temperature to be $\pm 10^{\circ}\text{C}$ for the various wind conditions. Although the maximum variation of the average
 198 temperature was set at $\pm 10^{\circ}\text{C}$, 90% of the cases are less than $\pm 5^{\circ}\text{C}$ and 80% of the cases are less than $\pm 3^{\circ}\text{C}$. The 10, 5 and 3 $^{\circ}\text{C}$ of error will give
 199 a maximum of 3.7%, 1.9% and 1.1% of error in power respectively. The cases with the large temperature difference are the cases with low wind
 200 speed and the hotter position away from the aperture. This is because the heat transfer between the hot air near the back of the cavity and ambient
 201 air is very low for the low wind speed condition.

202 **Table 2 list of setpoint temperature of each heater position for various conditions**

Temperature of the internal walls ($^{\circ}\text{C}$)		Wall position																
Temperature distribution		TA	TB	TC	TD	TE	TF	BA	BB	BC	BD	BE	BF	EA	EB	EC	ED	Average
Head-on $\alpha = 0^{\circ}$ $\varphi = 15^{\circ}$	Uniform	300	300	300	300	300	300	300	300	300	300	300	300	300	300	300	300	300
	Upper hotter	340	350	360	375	390	400	260	250	240	225	210	200	300	300	300	300	300
	Lower hotter	260	250	240	225	210	200	340	350	360	375	390	400	300	300	300	300	300
	Front hotter	275	250	250	300	350	400	250	225	250	300	350	400	300	300	300	300	300
	Rear hotter	350	400	325	275	250	225	350	400	325	275	225	200	300	300	300	300	300
Side-on $\alpha = 90^{\circ}$ $\varphi = 15^{\circ}$	Uniform	300	300	300	300	300	300	300	300	300	300	300	300	300	300	300	300	300
	Upper hotter	340	350	360	375	390	400	260	250	240	225	210	200	300	300	300	300	300
	Front hotter	275	250	250	300	350	400	250	225	250	300	350	400	300	300	300	300	300
	Rear hotter	350	400	325	275	250	225	350	400	325	275	225	200	300	300	300	300	300
Beam-down $\alpha = N/A$ $\varphi = -90^{\circ}$	Uniform	300	300	300	300	300	300	300	300	300	300	300	300	300	300	300	300	300
	Front /near aperture hotter	250	250	250	300	350	400	250	250	250	300	350	400	300	300	300	300	300
	Rear /near back wall hotter	325	400	325	275	250	225	325	400	325	275	250	225	300	300	300	300	300

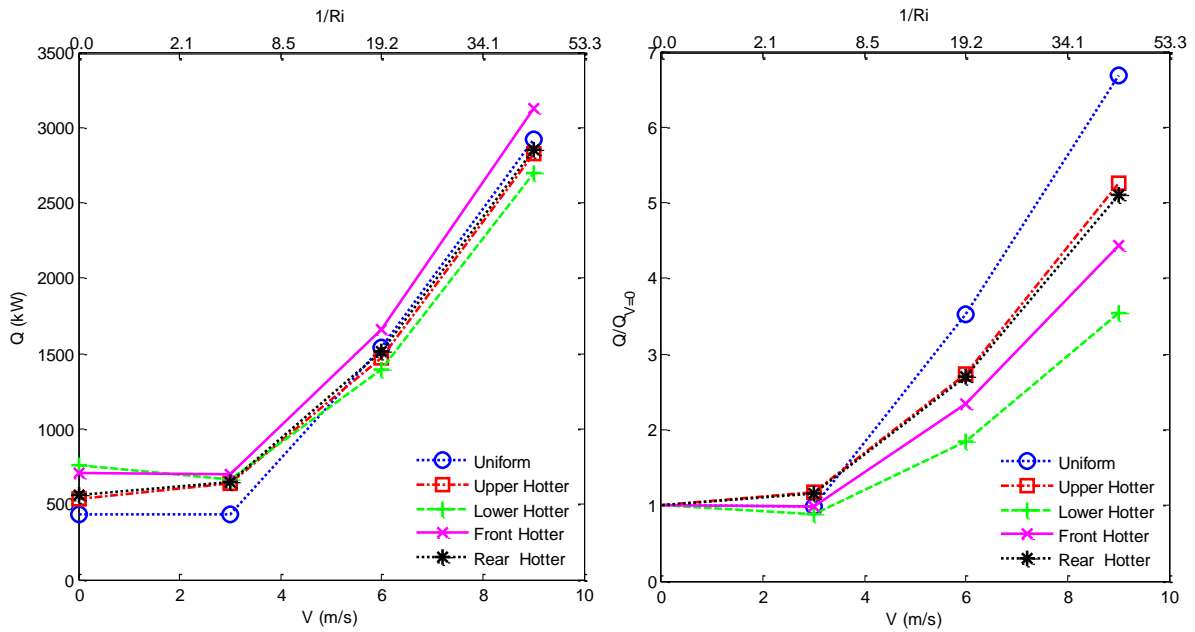
204 3 Results and discussion

205 3.1 Head-on wind

206 The effect of wind speed in the head-on direction, together with that of wall temperature
207 distribution on the convective heat losses through the aperture of a heated cavity is presented
208 in Figure 1. For low wind speed conditions ($Ri < 4.8$, $V < 3\text{m/s}$), the cases featuring the
209 ‘lower section hotter’ and ‘front section hotter’, have a higher convective heat loss than the
210 other cases, including that of the uniform distribution. The higher losses of the ‘lower section
211 hotter’ case, can be deduced to be associated with the added role of natural convection, that is
212 of buoyancy. The higher loss from the ‘front section hotter’ case suggest that close the
213 proximity of the hotter part of the wall to the aperture facilitates increased egress of the hot air
214 than for the reference case. Similarly, for high wind speed condition ($Ri > 19$, $V > 6\text{m/s}$), the
215 ‘front section hotter’ case has the highest measured value of the convective heat loss among all
216 the cases investigated. On the other hand, the ‘lower section hotter’ case features the lowest
217 convective heat loss for high wind speeds. This suggests that a greater fraction of the power
218 lost from the lower section is transferred under these conditions to maintain the temperature of
219 the upper and rear sections. Further evidence for this can be found from our previous study
220 (Lee et al. 2017), which identified a strong flow recirculation transporting the hot air from the
221 lower section toward the rear and the upper section before it leaves the cavity. This flow pattern
222 reduces that heat lost from the other surfaces, and hence the power required to maintain the set
223 point temperature of the lower temperature surface. Therefore, the qualitative trends from the
224 CFD (Lee et al. 2017) are consistent with the measured trend that the ‘lower section hotter’
225 case has the lowest convective heat loss behaviour of the cases assessed here for high wind
226 speed condition.

227 The dependence of the convective heat losses, normalised by the case for no wind on wind
228 speed is presented in Figure 2 for the same conditions as those reported in Figure 1. It can be
229 seen that varying the wall temperature distribution causes up to 50% change in the total natural
230 convection. The ‘upper section hotter’ case has the lowest convective heat loss where natural
231 convection dominates. For $V > 3\text{ m/s}$, the heat transfer moves to the mixed convection regime
232 which greatly reduces this range to $< 20\%$. Consistent with this trend, the ‘lower section hotter’
233 case has the highest loss for the lower wind speed case and lowest loss for high wind speed.
234 However, the ‘upper section hotter’ case has the lowest average convective heat loss in the
235 range of wind speeds investigated. For the cases with $V > 6\text{ m/s}$ the heat loss plateaus and
236 tends to become independent of the temperature distribution, which also implies that it tends
237 toward that of the uniform temperature distribution case. That is, the shape of the temperature
238 distribution becomes relatively unimportant in the inertia-dominated regime.

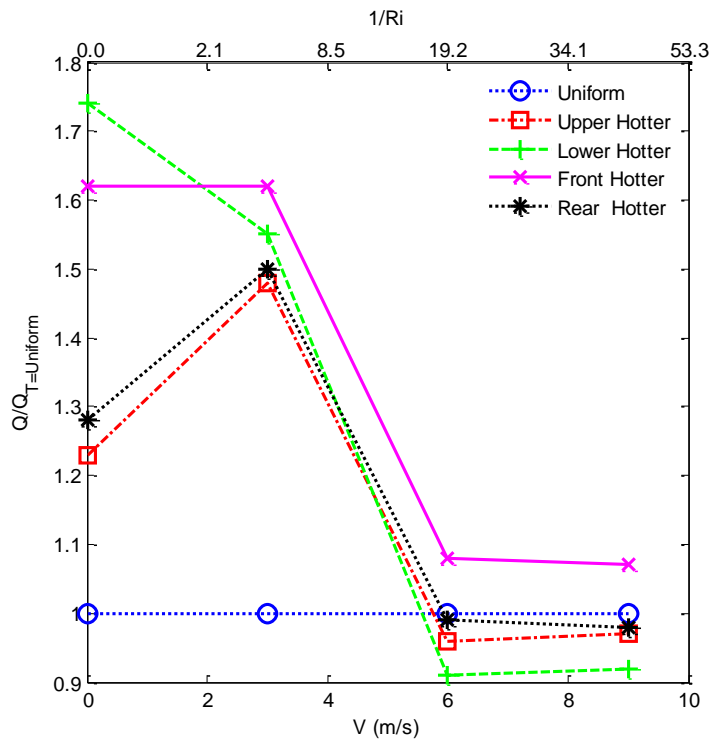
239



240

241
242

Figure 1 Dependence of the heat losses through the aperture on wind speed for a series of wall temperature distributions. Conditions: tilt angle of 15° , yaw angle of 0° , aperture ratio of 0.5 and aspect ratio of 1.5.



243

244
245

Figure 2 Dependence of the normalised heat losses through the aperture in wind speed for a series of wall temperature distributions. Conditions: tilt angle of 15° , yaw angle of 0° , aperture ratio of 0.5 and aspect ratio of 1.5.

246

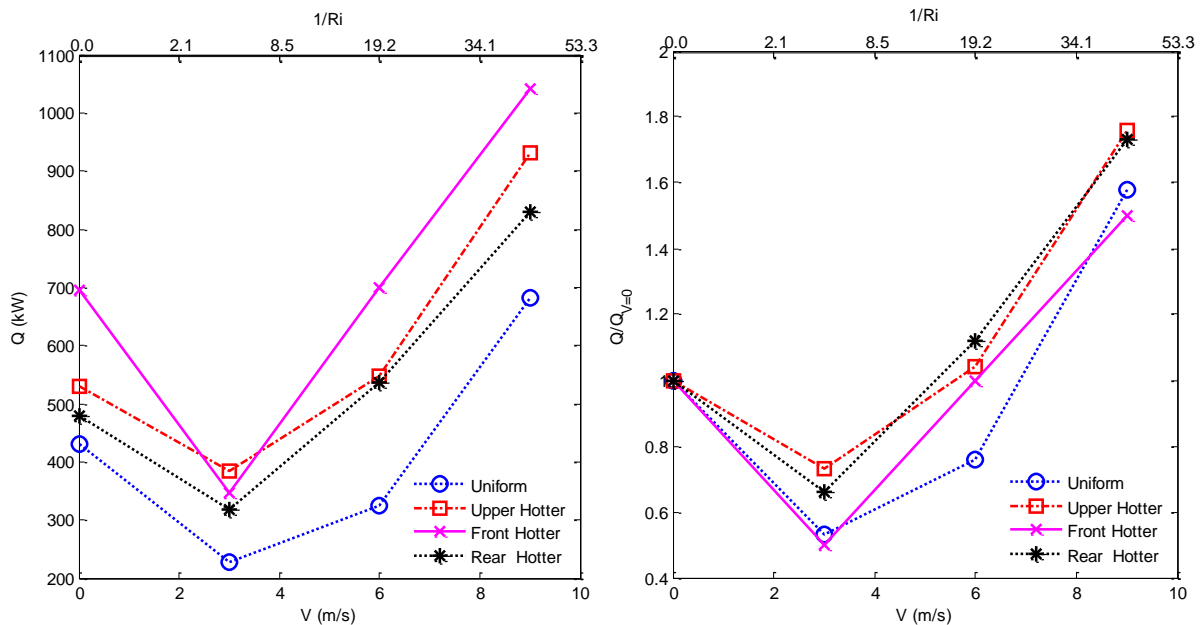
247 3.2 Side-on wind

248 The influence of wind speed on the convective heat losses through the aperture for the side-on
249 direction is presented in Figure 3 for several types of wall temperature distribution. The ‘front

250 section hotter' case has the highest convective heat loss for most of the cases, similar to the
 251 head-on wind cases. However, the 'rear section hotter' cases feature the lowest convective heat
 252 loss, which is different from the head-on wind cases. This can be attributed to the fact that the
 253 relatively cold wind does not penetrate as far into the cavity for the transverse direction as for
 254 the head-on direction. This deduction is reasonable for this configuration in which the cavity
 255 has an aspect ratio of 1.5 and an aperture ratio of 0.5 so that the distance between the aperture
 256 and the back section is 3 times that of the aperture diameter. Hence the 'rear section hotter'
 257 case is likely to have the lowest heat loss for those configurations in which a relatively
 258 quiescent zone is established at the rear of the chamber.

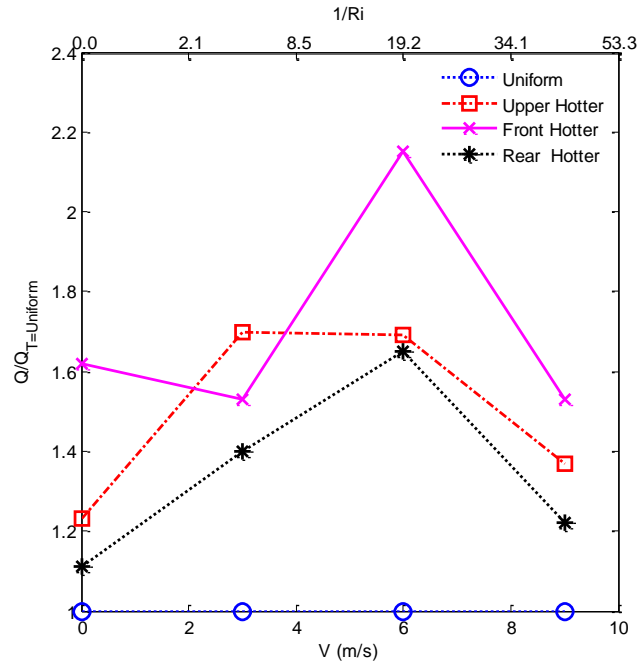
259 Figure 4 presents the same data as Figure 3, except that convective heat losses is normalised
 260 by the reference case of uniform wall temperature. This highlights the importance of wind
 261 speed on the effect of temperature distribution on the normalised convective heat loss. The
 262 'rear section hotter' case has ~40% less convective heat losses than does the distribution with
 263 the highest convective loss for all wind speeds assessed here.

264 Figure 4 also shows that the convective heat losses, which occur in the low wind speed range
 265 ($0 < V < 6 \text{ m/s}$, $0 < Ri < 19$) are less than the natural convection. This trend can be attributed
 266 to the generation by a side-on wind of a natural "aerodynamic seal" or "air curtain", which
 267 helps to mitigate the heat loss from the cavity. However, for $V > 6 \text{ m/s}$, the momentum of the
 268 transverse flow becomes so strong that it drives a mixing process between the cold wind and
 269 hot air inside the cavity that dominates of the "air curtain". Therefore, the convective heat loss
 270 increases strongly with the wind speed, for $V > 6 \text{ m/s}$.



271

272 **Figure 3** Dependence of the heat losses through the aperture on wind speed for a series of wall temperature
 273 distributions. Conditions: tilt angle of 15° , yaw angle of 90° , aperture ratio of 0.5 and aspect ratio of 1.5.



274

275 **Figure 4** Dependence of the normalised heat losses through the aperture on wind speed for a series of wall temperature
 276 distributions. Conditions: tilt angle of 15° , yaw angle of 90° , aperture ratio of 0.5 and aspect ratio of 1.5.

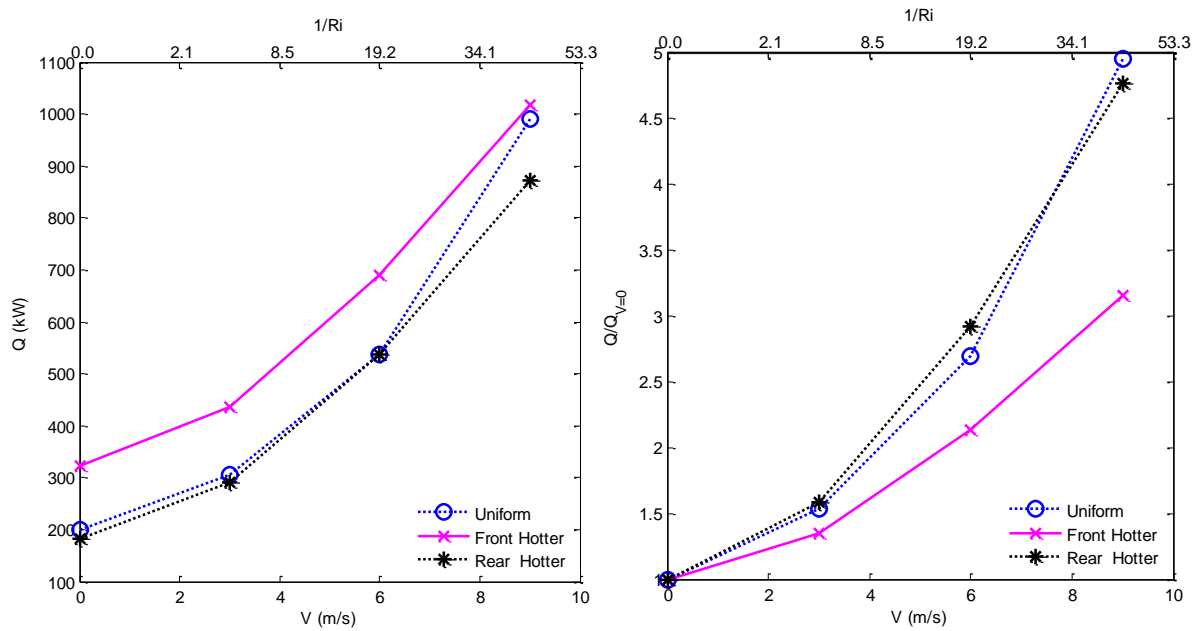
277

278 3.3 Upward facing cavity

279 The influence of wind speed on the convective heat losses through the aperture of an upward
 280 facing heated cavity is presented in Figure 5 for three different wall temperature distribution.
 281 The convective heat loss through the aperture increases non-linearly with the wind speed, and
 282 the case with the hotter surface near to the aperture has the highest heat losses through the
 283 aperture, which is consistent with the other cases. The heat losses through the aperture for the
 284 ‘near aperture hotter’ cases are approximately 150W higher than the ‘back wall hotter’ cases
 285 for all tested wind conditions. It is noteworthy that the wind speed has a particularly strong
 286 influence for the upward facing cavity. The convective power losses increase by approximately
 287 50% when the wind speed is increased from 0 to 3 m/s (Ri from 0 to 4.8). For the high wind
 288 speed condition ($Ri > 43, V > 9\text{m/s}$), the heat losses are ~ 5 times greater than the natural
 289 convection cases. The upward facing solar cavity receiver is also likely to place closer to the
 290 ground than the tower mounted case, where it is less windy than the downward facing cavity,
 291 which will further reduce the convective heat loss. In addition, the influence of wind is likely
 292 to be easier to mitigate by shielding for an upward facing cavity than a tilted one, since the
 293 wind direction is always normal to the cavity axis for the vertical orientation but varies in three
 294 dimensions for the tilted case.

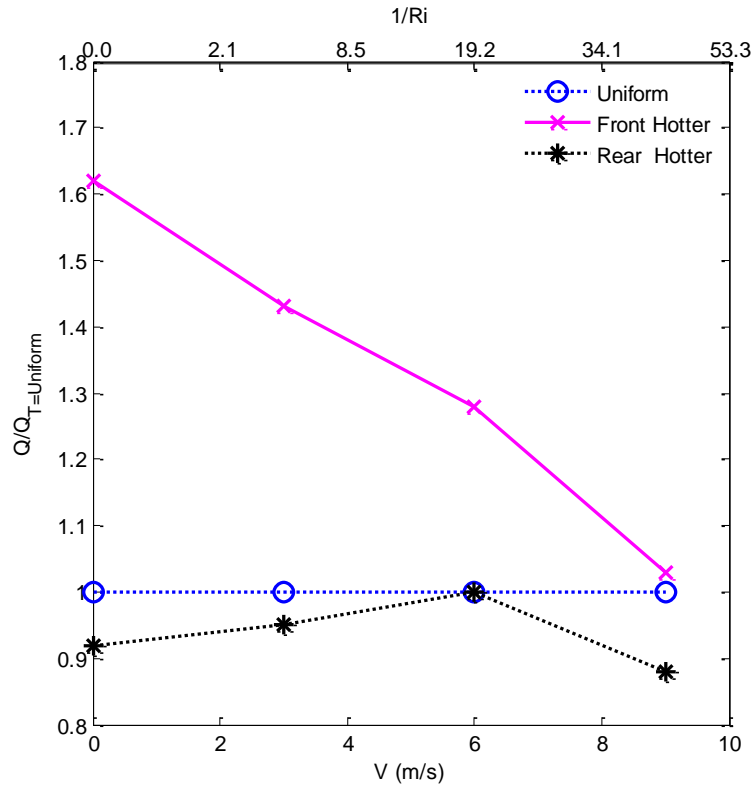
295 In contrast to Figure 3 in which the side-on wind was found to initially decrease convective
 296 losses for the tilted receiver, this reduction does not occur for the vertical orientation although
 297 the wind direction is also perpendicular to the aperture. This is consistent with the vertical
 298 orientation avoiding the strong adverse mechanism of the near horizontal orientations in which
 299 natural convection establishes a strong recirculation through the aperture.

300 Figure 6 presents for the vertical orientation the convective heat losses for the three temperature
 301 distributions normalised by the case with the uniform wall temperature. The shape of the
 302 temperature distribution can be seen to change the total convective heat losses by up to ~ 60%,
 303 which is more significant than the tilted cases. However, the impact of the shape of the
 304 temperature distribution decreases with an increase in wind speed to less than 20% for high
 305 wind speed condition ($Ri > 43, V > 9 \text{ m/s}$). The total convective heat losses converge with
 306 an increase in wind speed to a value that approaches the uniform temperature distribution case.
 307 This gives further evidence that both the orientation and temperature distribution become
 308 unimportant at sufficiently high wind speeds aligned normal to the cavity axis.



309

310 **Figure 5** Dependence of the heat losses and normalised heat loss wind speed through the aperture on wind speed for a
 311 series of wall temperature distributions. Conditions: tilt angle of -90° , yaw angle of 0° , aperture ratio of 0.5 and aspect
 312 ratio of 1.5.



313

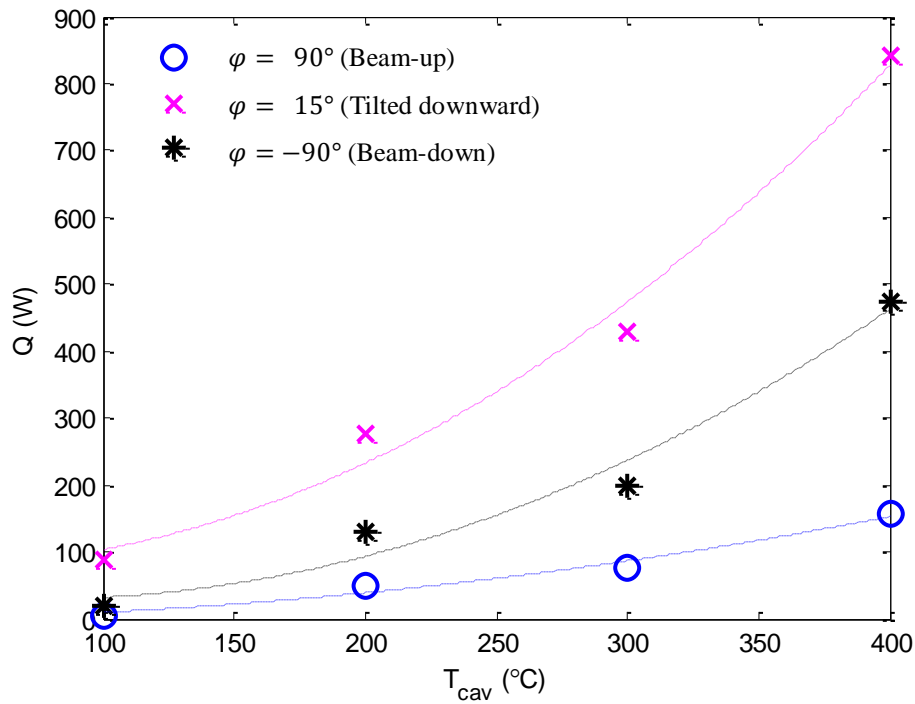
314 **Figure 6** Dependence of the normalised heat losses through the aperture on wind speed for a series of wall temperature
 315 distributions. Conditions: tilt angle of -90° , yaw angle of 0° , aperture ratio of 0.5 and aspect ratio of 1.5.

316

317 **3.4 Temperature and tilt angle**

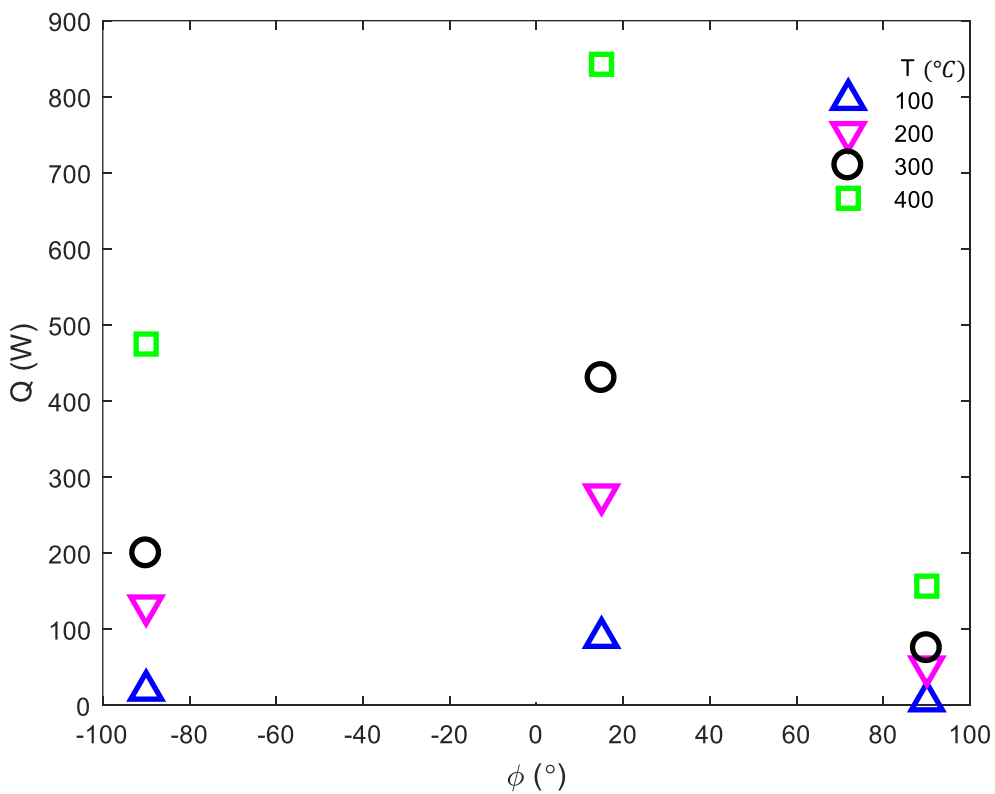
318 The combined effects of temperature and tilt angle of a heated cavity on convective heat losses
 319 through the aperture of a heated cavity are present in Figure 7, incorporating both the beam up
 320 ($\varphi = 90^\circ$) and beam down ($\varphi = -90^\circ$) cases. It can be seen that the beam-up has the lowest
 321 convection losses as expected, being only 30-40% that of the beam-down. Also the heat loss
 322 through the aperture increase non-linearly with temperature. This effect, which is observed fir
 323 all of the tested tilt angles cases, appears to be related to the influence of radiation heat loss,
 324 which has a fourth order dependence on temperature. Worth noting is that the heat loss from
 325 the aperture has a complex dependence on tilt angle. The heat losses from the 15° tilted cavity
 326 are higher than both the 90° and -90° cases. This indicates that there is at least one tilt angle
 327 which will have the highest convective heat loss, although further work in required to determine
 328 this. However, this angle is likely to also depend on the cavity dimensions. That is, the heat
 329 loss from the $\varphi = -90^\circ$ case may not necessarily be less than the 15° for all geometries, but is
 330 expected to depend on the geometry of the cavity, such as aspect ratio and aperture ratio (Bilgen
 331 & Oztop 2005). However, the trend is independent temperature, because the same trend can
 332 be observed in Figure 7a for all tested temperatures.

a)



333

b)



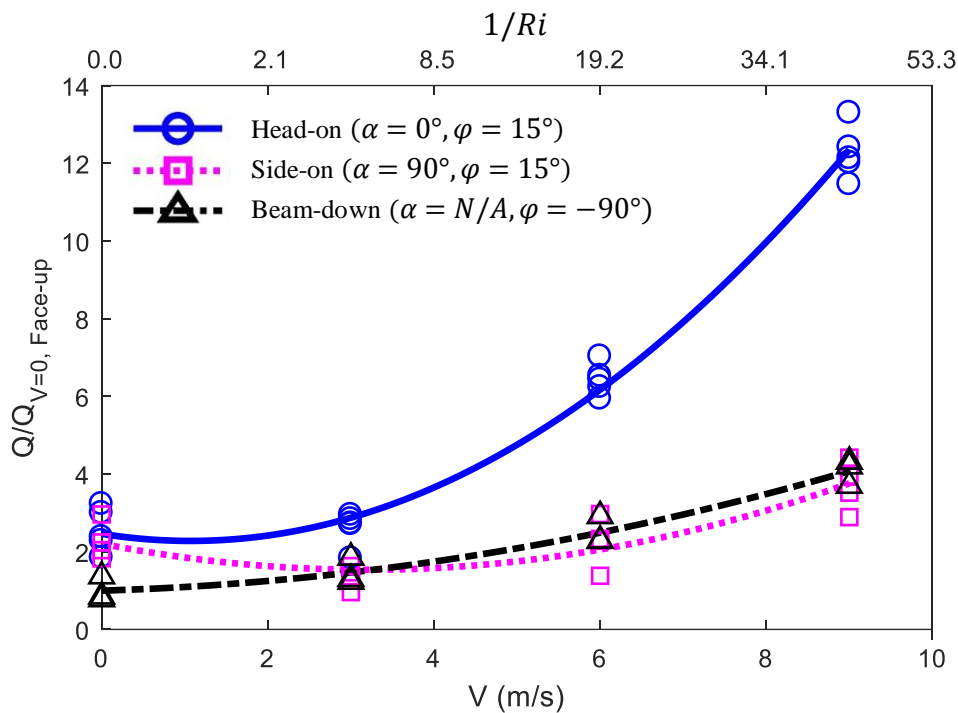
334

335 **Figure 7** Dependence of the heat losses through the aperture of a heated cavity on temperature and tilt angle.
 336 **Conditions:** no wind, aperture ratio of 0.5 and aspect ratio of 1.5.

337

338 The effect of wind speed on normalised heat losses by natural convection for the beam-down
 339 case, for various wind directions and the tilt angles is presented in Figure 8. The natural

340 convection of the ‘beam-down’ was chosen to be the reference case because it has the lowest
 341 heat losses. The figure shows that the ‘downward tilted cavity with side-on wind’ case has a
 342 very similar trend with the ‘beam-down’ case for wind speed $Ri > 4.8$. This is because, for
 343 both cases, the air/ wind flows parallel to the aperture plane. Therefore the flow pattern is
 344 expected to be similar for all wind speeds. For these 2 conditions, the increase in heat losses at
 345 high wind speed ($Ri < 43$) is up to 4.5 times the value of the natural convection of the ‘beam-
 346 down’ case. However, the influence of wind speed on heat losses through the aperture is very
 347 high for the head-on wind speed cases, to reach up to 12 times that of the reference case. This
 348 highlights the potential benefits of being able to mitigate convective heat loss from for head-
 349 on wind directions.

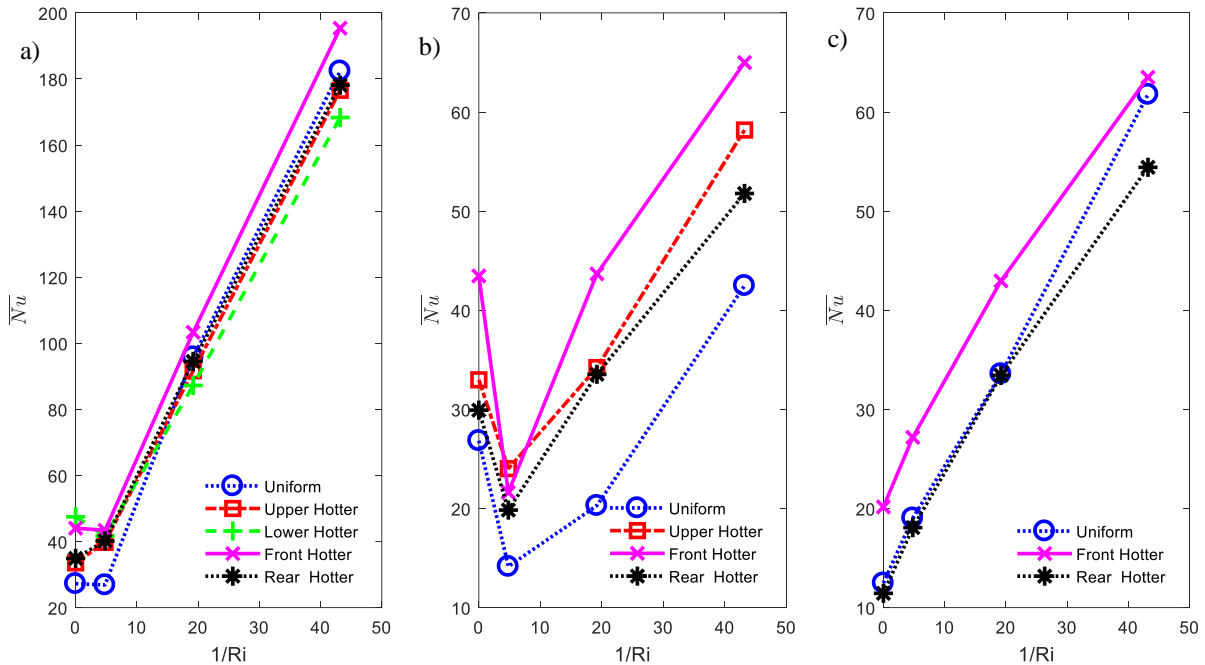


350

351 **Figure 8** Dependence of the normalised heat losses by natural convection of the ‘beam-down’ case on wind speed for a
 352 series of tilt and yaw angles. Conditions: aperture ratio of 0.5 and aspect ratio of 1.5.

353 The dependence of the inverse of Richardson number on the Nusselt number is presented in
 354 Figure 9 for three orientation. It can be seen that the data all collapse very well for the head-on
 355 case and quite well for the beam-up case, but is much more complex for the side-on orientation.
 356 A strong local minimum in the heat losses at $1/Ri \sim 5$ is clearly observed for of the side-on
 357 direction and a very weak minimum is present for a few cases in the head-on direction. This
 358 shows that a low velocity cross-flow can inhibit the buoyancy-driven transport of gas through
 359 the aperture when the cavity is tilted slightly downward. However, for an upward facing cavity,
 360 there is no stagnant zone so that a slight wind does not inhibit buoyancy for this case. Worth
 361 noting is that the heat losses from the head-on wind speed case does not vary much between
 362 the first 2 data points. Insufficient data are available to identify whether or not a local minimum
 363 or maximum is present between $0 < Ri < 5$. In addition, it is also noted that, for high wind
 364 speed the heat losses from the head-on cases are about 4 times larger than the side-on cases,
 365 agreeing with our earlier study (Lee et al. 2018a). The data also suggests that there may be a

366 local minimum at $1/Ri \sim 1.25$ for the head-on cases. Figure 9a also shows that, Nu has near
 367 linear dependency relationship with $1/Ri$ for $1/Ri > 10$ for the head-on case, hence this
 368 behaviour is also expected $1/Ri > 40$ for the side-on cases.



369

370 **Figure 9** Dependence of the Nusselt number of a heated cavity on the inverse of Richardson number for a series of
 371 wall temperature distributions. Conditions: aperture ratio of 0.5, aspect ratio of 1.5, a) head-on ($\alpha = 0^\circ$ and $\varphi =$
 372 15°), b) side-on ($\alpha = 90^\circ$ and $\varphi = 15^\circ$) and c) beam-down ($\alpha = N/A$ and $\varphi = -90^\circ$).

373 4 Conclusions

374 The dependence of convective heat loss on wind speed, yaw angle, tilt angle and temperature
 375 distribution from a cavity receiver of various geometrical parameters were investigated
 376 experimentally in this study. Results point to a complex and joint relationship between the heat
 377 loss and the various operating parameters. It is found that there is no heat flux profile that
 378 exhibits the best or worst convective heat flux for all orientation. In general, the heat losses
 379 from a downward tilted solar cavity receiver ($\varphi = 15^\circ$) tend to be minimised with the upper or
 380 rear surface to be hottest. This outcome should be further investigated with the solar optical
 381 system.

382 The convective losses are lowest for the beam-up orientation as expected, but the downward
 383 tilted solar cavity receiver ($\varphi = 15^\circ$) has greater losses than the beam down, even at zero
 384 wind, which contradicts the expectation from the literature. The main reason for this difference
 385 is that the wind direction is always normal to the cavity for the beam-up and beam-down
 386 orientations, which is the orientation with the lowest convective losses. These configurations
 387 avoid the wind flowing directly into the cavity, which has the greatest connective losses.
 388 Furthermore, at high wind speeds, with corresponds to high inverse Richardson number, the
 389 heat transfer is momentum dominated, so that the heat losses are controlled by orientation
 390 relative to the wind, irrespective of the direction of gravity.

391 Finally, the heat loss from a beam down cavity receiver has a nearly linear dependence on $1/Ri$
392 throughout the range. This linear dependence shows that natural convection is not significant
393 anywhere. For the downward tilted orientation, the relationship becomes linear for higher wind
394 speed, where momentum dominates over natural convection. The study also suggested that
395 there may be a local minimum of heat loss at $1/Ri \sim 1.25$ for the head-on cases. However, this
396 wind speed is out of the range of the wind tunnel of this study, so requires further work to
397 confirm.

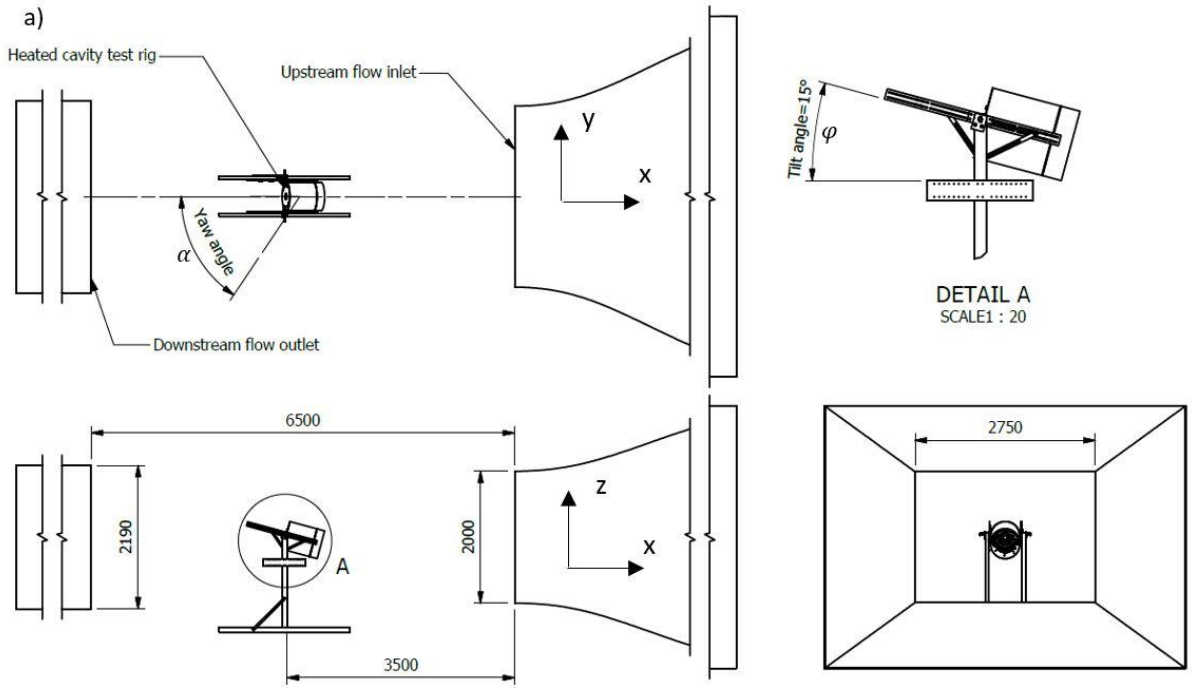
398

399 **Acknowledgements**

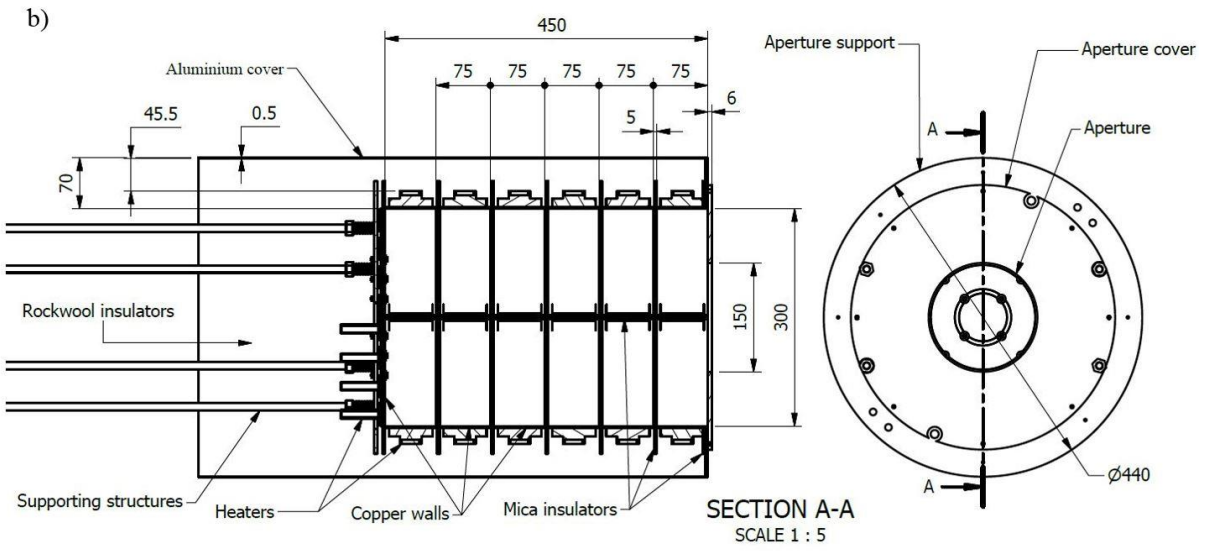
400 This research has been financed by the Australian Renewable Energy Agency (ARENA) and
401 the University of Adelaide, through the Australian Solar Thermal Research Initiative (ASTRI),
402 ARENA1-SRI002.

403

404 **Supplement**



405



406

407 **Figure S1 Schematic diagram of a) the heated cavity in the Thebarton wind tunnel and b) the dimensions of the receiver.**

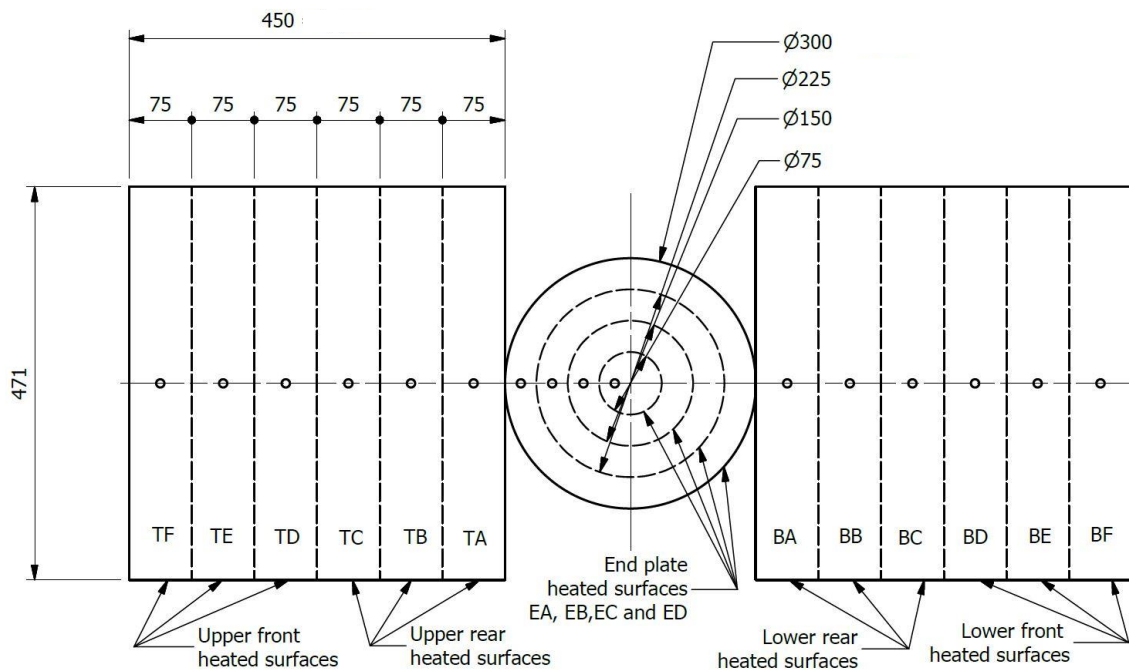
408

409

410

411

412



413

414

415

416

Figure S2 Schematic diagram of the simplified configuration of the internal copper wall surface of the heated cavity (shown unrolled view). The thermocouples are shown as small circles. Please notice that, for the cavity facing upward cases (tilt angle = -90°), upper heaters are the downstream heaters and lower heaters are the upstream heaters.

417

418

Table 3 List of instrumentation/ uncertainty term

Instrumentation/ uncertainty term	Accuracy/ uncertainty
K-type thermocouple	$\pm 2.2^\circ\text{C} / \pm 0.7\%$
Datataker DT85	$\pm 0.01\%$
Arduino with DMX output	$\pm 0.2\%$
Lighting system power controllers	$\pm 1.5\%$
Steady state temperature	$\pm 0.5^\circ\text{C} / \pm 0.2\%$
Steady state power	$\pm 0.5\%$

419

420 References

421

422

423

Asselineau, C-A, Abbassi, E & Pye, J 2014, 'Open cavity receiver geometry influence on radiative losses', in *Proceedings of Solar2014, 52nd Annual Conference of the Australian Solar Energy Society, Solar2014, ed.(Melbourne, 2014).*

424

425 ASTRI 2017, *ASTRI Milestone 12 Report- For Public Dissemination*, Australian Solar
426 Thermal Research Initiative, <[http://www.astri.org.au/wp-content/uploads/2018/04/iii-
427 ASTRI-M12-2017-Public-Dissemination-Report.pdf](http://www.astri.org.au/wp-content/uploads/2018/04/iii-ASTRI-M12-2017-Public-Dissemination-Report.pdf)>.

428

429 Bilgen, E & Oztop, H 2005, 'Natural convection heat transfer in partially open inclined square
430 cavities', *International Journal of Heat and Mass Transfer*, vol. 48, no. 8, pp. 1470-1479.

431

432 Chinnici, A, Arjomandi, M, Tian, Z & Nathan, G 2016, 'A novel solar expanding-vortex
433 particle reactor: experimental and numerical investigation of the iso-thermal flow field and
434 particle deposition', *Solar energy*, vol. 133, pp. 451-464.

435

436 Chinnici, A, Arjomandi, M, Tian, ZF, Lu, Z & Nathan, GJ 2015, 'A novel solar expanding-
437 vortex particle reactor: influence of vortex structure on particle residence times and
438 trajectories', *Solar energy*, vol. 122, pp. 58-75.

439

440 Chinnici, A, Nathan, G & Dally, B 2018a, 'Experimental demonstration of the hybrid solar
441 receiver combustor', *Applied Energy*, vol. 224, pp. 426-437.

442

443 Chinnici, A, Nathan, G & Dally, B 2018b, 'An experimental study of the stability and
444 performance characteristics of a Hybrid Solar Receiver Combustor operated in the MILD
445 combustion regime', *Proceedings of the Combustion Institute*.

446

447 Clausing, A 1983, 'Convective losses from cavity solar receivers—comparisons between
448 analytical predictions and experimental results', *Journal of Solar Energy Engineering*, vol. 105,
449 no. 1, pp. 29-33.

450

451 Flesch, R, Stadler, H, Uhlig, R & Hoffschmidt, B 2015, 'On the influence of wind on cavity
452 receivers for solar power towers: An experimental analysis', *Applied thermal engineering*, vol.
453 87, pp. 724-735.

454

455 Flesch, R, Stadler, H, Uhlig, R & Pitz-Paal, R 2014, 'Numerical analysis of the influence of
456 inclination angle and wind on the heat losses of cavity receivers for solar thermal power
457 towers', *Solar energy*, vol. 110, pp. 427-437.

458

459 Gil, R, Monné, C, Bernal, N, Muñoz, M & Moreno, F 2015, 'Thermal Model of a Dish Stirling
460 Cavity-Receiver', *Energies*, vol. 8, no. 2, pp. 1042-1057.

461

462 Ho, CK & Iverson, BD 2014, 'Review of high-temperature central receiver designs for
463 concentrating solar power', *Renewable and Sustainable Energy Reviews*, vol. 29, pp. 835-846.

464

465 Holman, J 1997, 'Heat transfer', 8th edn, McGraw-Hill, New York.

466
467 Hu, T, Jia, P, Wang, Y & Hao, Y 2017, 'Numerical simulation on convective thermal loss of a
468 cavity receiver in a solar tower power plant', *Solar energy*, vol. 150, pp. 202-211.

469
470 Kolb, GJ, Ho, CK, Mancini, TR & Gary, JA 2011, 'Power tower technology roadmap and cost
471 reduction plan', *Sandia National Laboratories, Livermore, CA, Technical Report No.*
472 *SAND2011-2419*.

473
474 Lee, KL, Chinnici, A, Jafarian, M, Arjomandi, M, Dally, B & Nathan, G 2018a, 'Experimental
475 investigation of the effects of wind speed and yaw angle on heat losses from a heated cavity',
476 *Solar energy*, vol. 165, pp. 178-188.

477
478 Lee, KL, Chinnici, A, Jafarian, M, Arjomandi, M, Dally, B & Nathan, G 2018b, 'Experimental
479 investigation of the effects of wind speed, aperture ratio and tilt angle on the heat losses from
480 a heated cavity', *Solar energy*, vol. under review.

481
482 Lee, KL, Jafarian, M, Ghanadi, F, Arjomandi, M & Nathan, GJ 2017, 'An investigation into
483 the effect of aspect ratio on the heat loss from a solar cavity receiver', *Solar energy*, vol. 149,
484 pp. 20-31.

485
486 Leonardi, E 2012, 'Detailed analysis of the solar power collected in a beam-down central
487 receiver system', *Solar energy*, vol. 86, no. 2, pp. 734-745.

488
489 Li, X, Dai, Y & Wang, R 2015, 'Performance investigation on solar thermal conversion of a
490 conical cavity receiver employing a beam-down solar tower concentrator', *Solar energy*, vol.
491 114, pp. 134-151.

492
493 Ma, RY 1993, *Wind effects on convective heat loss from a cavity receiver for a parabolic*
494 *concentrating solar collector*, Sandia National Laboratories.

495
496 Mokhtar, M 2011, 'The beam-down solar thermal concentrator: experimental characterization
497 and modeling', Master's Thesis. Masdar Institute of Science and Technology, Abu Dhabi,
498 United Arab Emirates.

499
500 Mokhtar, M, Meyers, SA, Armstrong, PR & Chiesa, M 2014, 'Performance analysis of masdar
501 city's concentrated solar beam-down optical experiment'.

502
503 Paitoonsurikarn & Lovegrove, K 2003, 'On the study of convection loss from open cavity
504 receivers in solar paraboloidal dish applications', in *Proceedings of 41st Conference of the*
505 *Australia and New Zealand Solar Energy Society (ANZSES), Melbourne, Australia*.

506

507 Paitoonsurikarn, S & Lovegrove, K 2002, 'Numerical investigation of natural convection loss
508 in cavity-type solar receivers', in *Proceedings of Solar*.

509

510 Paitoonsurikarn, S, Lovegrove, K, Hughes, G & Pye, J 2011, 'Numerical investigation of
511 natural convection loss from cavity receivers in solar dish applications', *Journal of Solar*
512 *Energy Engineering*, vol. 133, no. 2, p. 021004.

513

514 Philibert, C 2010, *Technology roadmap: concentrating solar power*, OECD/IEA.

515

516 Sánchez-González, A, Rodríguez-Sánchez, MR & Santana, D 2016, 'Aiming strategy model
517 based on allowable flux densities for molten salt central receivers', *Solar energy*.

518

519 Segal, A & Epstein, M 2008, 'Practical considerations in designing large scale “beam down”
520 optical systems', *Journal of Solar Energy Engineering*, vol. 130, no. 1, p. 011009.

521

522 Stalin Maria Jebamalai, J 2016, 'Receiver Design Methodology for Solar Tower Power Plants'.

523

524 Steinfeld, A & Schubnell, M 1993, 'Optimum aperture size and operating temperature of a solar
525 cavity-receiver', *Solar energy*, vol. 50, no. 1, pp. 19-25.

526

527 Tanaka, N 2010, 'Technology Road Map, Concentrating Solar Power', *International Energy*
528 *Agency*.

529

530 Taumoefolau, T, Paitoonsurikarn, S, Hughes, G & Lovegrove, K 2004, 'Experimental
531 investigation of natural convection heat loss from a model solar concentrator cavity receiver',
532 *Journal of Solar Energy Engineering*, vol. 126, no. 2, pp. 801-807.

533

534 Wei, X, Lu, Z, Yu, W & Xu, W 2013, 'Ray tracing and simulation for the beam-down solar
535 concentrator', *Renewable Energy*, vol. 50, pp. 161-167.

536

537 Wu, S-Y, Shen, Z-G, Xiao, L & Li, D-L 2015, 'Experimental study on combined convective
538 heat loss of a fully open cylindrical cavity under wind conditions', *International Journal of*
539 *Heat and Mass Transfer*, vol. 83, pp. 509-521.

540

541 Wu, S-Y, Xiao, L, Cao, Y & Li, Y-R 2010, 'Convection heat loss from cavity receiver in
542 parabolic dish solar thermal power system: a review', *Solar energy*, vol. 84, no. 8, pp. 1342-
543 1355.

544

545 Wu, S-Y, Xiao, L & Li, Y-R 2011, 'Effect of aperture position and size on natural convection
546 heat loss of a solar heat-pipe receiver', *Applied thermal engineering*, vol. 31, no. 14, pp. 2787-
547 2796.

548

549 Xiao, L, Wu, S-Y & Li, Y-R 2012, 'Numerical study on combined free-forced convection heat
550 loss of solar cavity receiver under wind environments', *International Journal of Thermal*
551 *Sciences*, vol. 60, pp. 182-194.

552

553

554